Nuclear Engineering and Technology 51 (2019) 702–708

Contents lists available at ScienceDirect

Nuclear Engineering and Technology

journal homepage: www.elsevier.com/locate/net

Original Article

Real-time estimation of break sizes during LOCA in nuclear power plants using NARX neural network

Mahdi Saghafi [a, *], Mohammad B. Ghofrani [b]

[a] Department of Mechanical Engineering, University of Bonab, Bonab, Iran
[b] Department of Energy Engineering, Sharif University of Technology, Tehran, Iran

ARTICLE INFO

Article history:
Received 7 May 2018
Received in revised form
1 November 2018
Accepted 29 November 2018
Available online 29 November 2018

Keywords:
Break size estimation
Loss of coolant accident
NARX neural network
Nuclear power plants
Accident management support tools

ABSTRACT

This paper deals with break size estimation of loss of coolant accidents (LOCA) using a nonlinear autoregressive with exogenous inputs (NARX) neural network. Previous studies used static approaches, requiring time-integrated parameters and independent firing algorithms. NARX neural network is able to directly deal with time-dependent signals for dynamic estimation of break sizes in real-time. The case studied is a LOCA in the primary system of Bushehr nuclear power plant (NPP). In this study, number of hidden layers, neurons, feedbacks, inputs, and training duration of transients are selected by performing parametric studies to determine the network architecture with minimum error. The developed NARX neural network is trained by error back propagation algorithm with different break sizes, covering 5% −100% of main coolant pipeline area. This database of LOCA scenarios is developed using RELAP5 thermal-hydraulic code. The results are satisfactory and indicate feasibility of implementing NARX neural network for break size estimation in NPPs. It is able to find a general solution for break size estimation problem in real-time, using a limited number of training data sets. This study has been performed in the framework of a research project, aiming to develop an appropriate accident management support tool for Bushehr NPP.

1. Introduction

Early failure detection and diagnosis play a fundamental role in safe and reliable operation of a nuclear power plant (NPP) [1–3]. NPP operators have to rapidly take appropriate actions to prevent an incident from developing to a severe accident or to mitigate accident consequences, which require complex judgments and trade-offs in stressful situations like Fukushima accident [4]. Hundreds of alarms within the first minute of emergency situations such as loss of coolant accidents (LOCA) in NPPs, may cause operator confusion [5]. Break size estimation is required for determining corrective actions to recover core heat removal after LOCAs, as well as prediction of leak flow rate [6], water level of reactor pressure vessel (RPV) [7], and timing of major events in LOCAs [8].

Break size estimation of LOCA in NPPs can be considered as an inverse problem, which can be solved by either model-based or model-free methods. EPRI [9] proposed an analytical model based on chocked-flow equations to estimate break sizes. Inputs of this model-based approach are thermodynamic parameters and depressurization rate of the NPP, which are calculated by operators. Model-free methods can be very helpful in reducing operator cognitive workload and easing decision making process. Various types of model-free methods such as artificial neural networks (ANN) [1,10,11], support vector regression (SVR) [12], and group method of data handling (GMDH) [13] have been applied for break size estimation in NPPs.

ANN is the best soft-computing approach for dealing with the problems with significantly overlapping patterns, dynamically changing environments, high background noise, and absence of accurate and fast models [14]. ANNs have been extensively implemented for fault detection and diagnosis of NPPs and their components [11]. Different types of ANNs can be trained to identify the states of complex systems such as NPPs. Feed-forward multilayer perceptron (MLP) with different training algorithms and architectures were used for break size estimation in NPPs, e.g. feed-water line break of a pressurized water reactor (PWR) [1], LOCA in

* Corresponding author.
E-mail address: msaghafi@bonabu.ac.ir (M. Saghafi).

https://doi.org/10.1016/j.net.2018.11.017

different locations of a pressurized heavy water reactor (PHWR) [4], and a PWR [11]. Feed-forward fuzzy neural networks (FNN) trained using genetic algorithm, were also applied to break size estimation in hot-leg, cold-leg, and steam-generator tubes of a PWR [10]. To the authors' knowledge, previous studies on break size estimation used static methods, which require independent firing algorithms and integrating of thermal-hydraulic (TH) parameters during the transient. In this study, a NARX neural network, which is able to directly deal with the time-dependent signals, has been applied for dynamic estimation of break sizes in the real-time.

The objective of the current study is to develop a NARX neural network, for break size estimation of LOCAs, which will be implemented in the structure of an accident management support tool (AMST) developed for Bushehr NPP [15–18]. AMSTs are used to ease decision making of the plant operators in selection of accident management countermeasures. AMSTs mainly consist of three parts, namely, Tracker, Predictor, and Decision support [8]. The Tracker enables operators to have insights into NPP states during accident management. A NARX neural network has been developed to be used for break size estimation in the Tracker. The break size estimation module of the Tracker is subdivided into: (1) a fuzzy classifier to categorize the break-type accidents in the primary system into three categories, i.e. LOCA in cold leg, LOCA in hot leg, and steam generator tube rupture (SGTR), and (2) three NARX neural networks to estimate break sizes in each category. The results provided by the break size estimation module are used whenever a break-type accident is identified. A set of modular ANNs is conceived to accident identification in the Tracker of the AMST. These modular ANNs continuously monitor the plant states and identify the initiating event of the accident, based on TH parameters of the NPP. The Trackers equipped with a NARX neural network, will provide more precise support in identification of break-type accidents during accident management.

The rest of the paper is arranged as follows: Section 2 gives a quick insight into NARX neural networks. The developed database for training, testing and validation process of the network for break size estimation in Bushehr NPP is briefly introduced in Section 3. In Section 4, the architecture of the NARX neural network, developed based on parametric studies, are presented. The results of NARX application are reported and discussed in Section 5. Section 6 ends the paper with some concluding remarks.

2. Description of NARX neural networks

By adding feedback connections to the architecture of feed-forward networks, recurrent neural networks (RNN) are formed, which are able to deal with temporal input signals. NARX neural networks, as a subcategory of RNNs, have limited feedbacks which come only from the output neurons rather the hidden neurons [19]. NARX model is a discrete-time nonlinear system as follows:

$$y(t) = f(y(t-1), \ldots, y(t-m),\ u(t),\ \ldots,\ u(t-p)) \quad (1)$$

where $u(t)$ and $y(t)$ are time-dependent input and output of the network at time t, p and m are the input-memory and output-memory order, and f is a nonlinear function [19]. NARX model is called a NARX neural network, when the function f is approximated by a MLP. Different training methods can be used in training process of the MLP of a NARX neural network. Training process is accomplished by adjusting the connecting weights of neurons to get the appropriate estimations. Gradient-descent learning is more effective in NARX neural networks than in other RNN architectures when applied to nonlinear system identification [20]. Also, NARX neural network with gradient-decent learning, converges much faster and can generalize better than RNN [21]. Flow chart of training process of the developed NARX neural network is presented in Fig. 1. In the training with gradient-descent method,

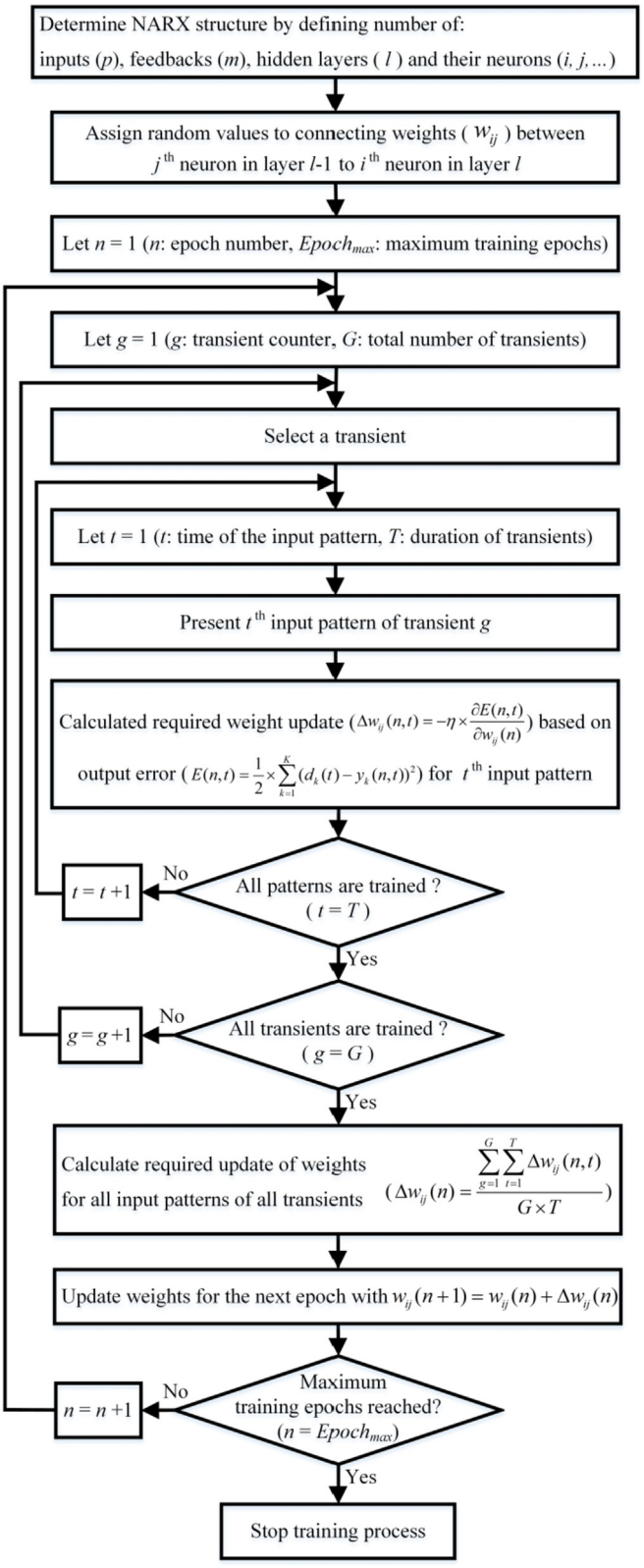

Fig. 1. Flow chart of training process of the developed NARX neural network.

weights of the network are successively adjusted by error back propagation (EBP) algorithm to minimize a quadratic cost function, which is defined as follows:

$$E(n,t) = \frac{1}{2} \times \sum_{k=1}^{K} (d_k(t) - y_k(n,t))^2 \quad (2)$$

where $d_k(t)$ and $y_k(n,t)$ are the actual and estimated values of kth output at time t in nth iteration, respectively. In this study, sigmoidal activation function is used for all neurons:

$$y(\alpha_i) = \tanh\left(\frac{\alpha_i}{2}\right) \quad (3)$$

where α_i is the total inputs of the ith neuron. Weight updating rule after any iteration, between jth neuron in layer $l-1$ and ith neuron in layer l is:

$$w_{ij}(n+1) = w_{ij}(n) + \Delta w_{ij}(n) \quad (4)$$

where $\Delta w_{ij}(n)$ is the required weight variation in nth iteration.

For batch learning of whole transient, updating of the weights is accomplished for all T data points of the transient at the same time. In addition, for training NARX neural network with different break sizes without losing previous learnings, all training transients should be involved in weight updating process in any iteration [21]. Therefore, the overall weight variation for G transients is calculated from (5).

$$\Delta w_{ij}(n) = \frac{\sum_{g=1}^{G} \sum_{t=1}^{T} \Delta w_{ij}(n,t)}{G \times T} \quad (5)$$

where $\Delta w_{ij}(n,t)$ is the weight difference calculated for any data set from (6) with learning rate of η.

$$\Delta w_{ij}(n,t) = -\eta \times \frac{\partial E(n,t)}{\partial w_{ij}(n)} \quad (6)$$

To have an overall estimation of errors for each transient, total transient squared error (TTSE) is defined from (7). Average TTSE is calculated by averaging for G transients.

$$TTSE = \frac{1}{2} \sum_{t=1}^{T} E(n,t) = \frac{1}{2} \times \sum_{t=1}^{T} \sum_{k=1}^{K} (d_k(t) - y_k(n,t))^2 \quad (7)$$

3. Development of a TH database for break size estimation in Bushehr NPP

Field measurement of TH parameters during LOCAs in NPPs should ideally be used in training process of NARX neural networks. Because of unavailability of plant specific data covering the whole range of break sizes, the database for training and testing process should be developed based on simulation of LOCAs with various sizes by appropriate TH codes. RELAP5 is a detailed TH code for accident analysis and its capability to accurately prediction of TH response of NPPs is validated in the literature [22]. As a case study to investigate the feasibility of using NARX neural network for break size estimation, 13 scenarios of LOCA with various break sizes (5%–100% of main pipeline area) in the cold leg of Bushehr NPP plus a null-transient scenario are modeled using RELAP5 code. Bushehr NPP is a four loop Russian-designed light water reactor, i.e. VVER-1000. RELAP5 nodalization of the developed TH model of Bushehr

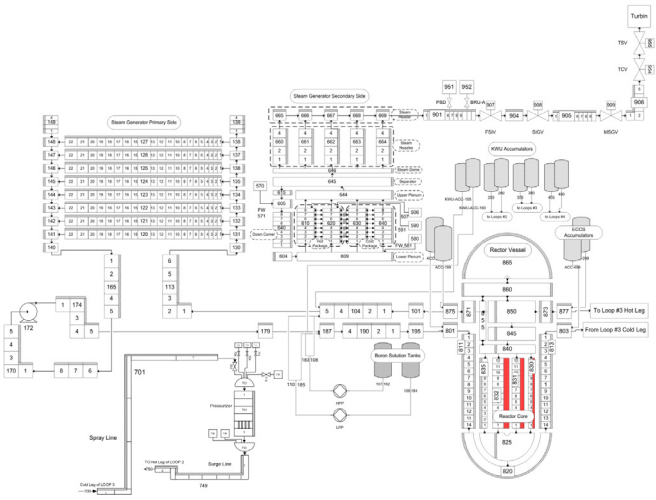

Fig. 2. Nodalization of the developed TH model for Bushehr NPP in RELAP5 code.

NPP is shown in Fig. 2. All break scenarios for this study are generated with availability of passive parts of emergency core cooling system (ECCS), i.e. accumulators, and unavailability of active parts of ECCS (low and high pressure injection systems). For 13 base scenarios, default Henry-Fauske critical flow model was used with default values for the discharge coefficient (1.0) and the thermal nonequilibrium constant (0.14). Time trend of RPV pressure for all cases of the database is presented in Fig. 3. First 100 s of all cases is dedicated to null-transient condition and then the break in the cold leg occurs. Generally, larger break sizes lead to faster depressurization of the primary system.

The developed database for training process of NARX neural network consists of a null-transient scenario plus 13 LOCA scenarios with different sizes ranging from 5% to 100% of cross sectional area of main coolant pipelines. For simulated scenarios, time evolution of the pressure inside RPV and the actual break size are used to generate the database.

Before starting the training process, all inputs of NARX neural network are scaled between −0.5 and 0.5 with (8), according to their minimum and maximum values. The scaling of the input data makes learning process easier, because the original data contained both small and large values [11].

$$x_{scaled} = \frac{x - \min(x)}{\max(x) - \min(x)} - 0.5 \quad (8)$$

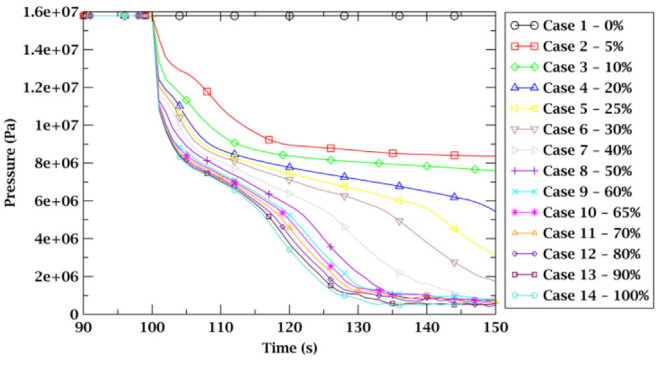

Fig. 3. Time trend of RPV pressure for all cases of the database.

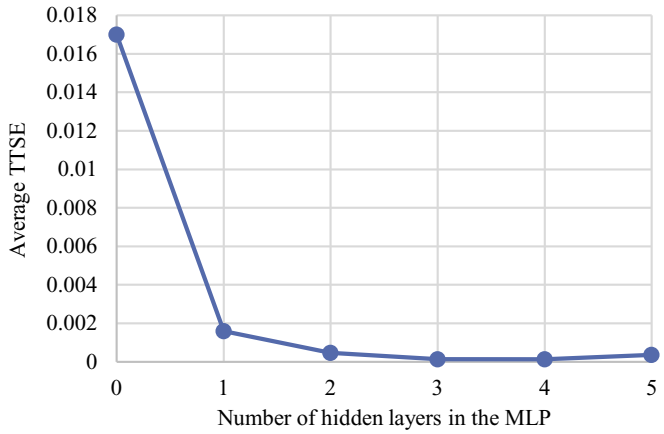

Fig. 4. Variation of average TTSE for training LOCA scenarios versus number of hidden layers of the MLP.

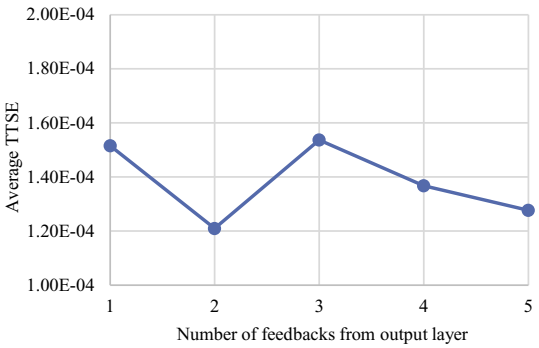

Fig. 6. Variation of average TTSE for training LOCA scenarios versus number of feedbacks from output layer.

4. Development and training of the NARX neural network

In case of LOCAs in a PWR NPP, pressure of the primary system starts to decrease as a time-dependent pattern. In this study, estimation of break sizes is based on pressure variations in the RPV during LOCAs. Time-dependent pressure signal at early phase of LOCAs are selected for training of NARX neural network, to increase the training speed and eliminate the effect of actuation of ECCS active part. The generated database has been partitioned in training, testing, and validation data sets. NARX neural network is trained by EBP algorithm using the training data sets. The validation data sets are used to overcome the over-fitting problem. Also, testing data sets are employed to verify the capability of NARX neural network to estimate break sizes, which are not used in the training process. Approximately 70% of transients in the database are selected for training, 15% for validation, and 15% are left for testing of NARX neural network.

Number of hidden layers, neurons, feedbacks, inputs, and training duration of transients are selected by performing parametric studies to determine the network architecture with the minimum error. Fig. 4 shows the variation of average TTSE for training LOCA scenarios versus number of hidden layers of the MLP in the NARX model. MLP with three hidden layers has the best learning performance to be implemented in the NARX model. Average TTSE of training data sets for different number of neurons in hidden layers of the MLP is illustrated in Fig. 5. Minimum error for training scenarios is achieved with a 10-20-10 structure of hidden layers in the MLP. Variation of average TTSE for different number of feedbacks from out layer to input layer of NARX neural network is presented in Fig. 6. It shows that NARX network with two feedbacks of the estimated break size has the minimum error for training data sets. In Fig. 7, variation of average TTSE for different number of inputs from the pressure signal is shown. Minimum error is achieved by patterns with 8 pressure points. Fig. 8 shows average TTSE versus different durations of the

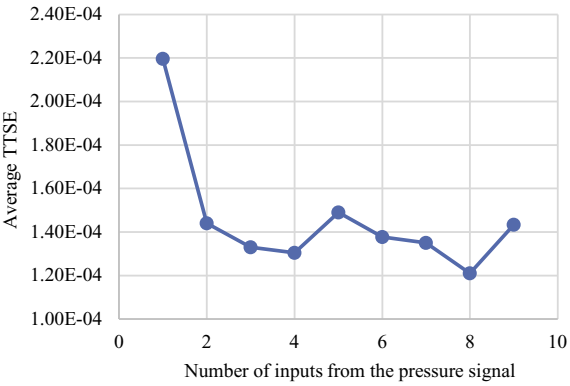

Fig. 7. Variation of average TTSE for training LOCA scenarios versus number of inputs from the pressure signal.

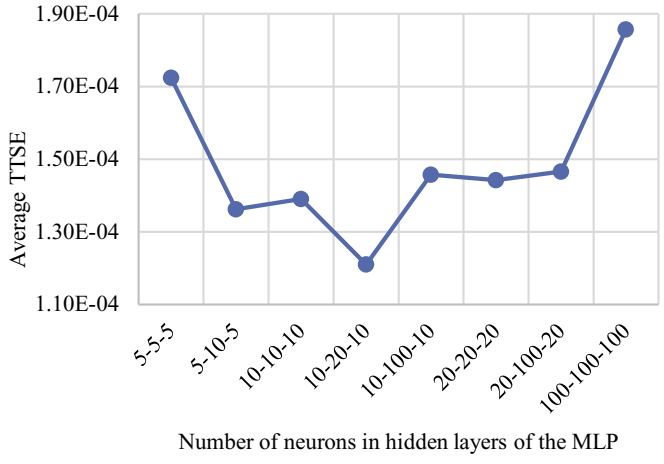

Fig. 5. Variation of average TTSE for training LOCA scenarios versus number of neurons in hidden layers of the MLP.

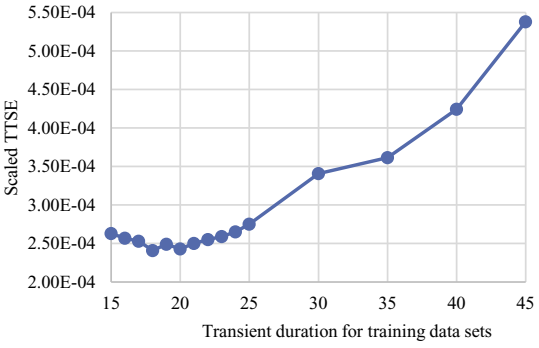

Fig. 8. Variation of average TTSE versus different duration of the training transients.

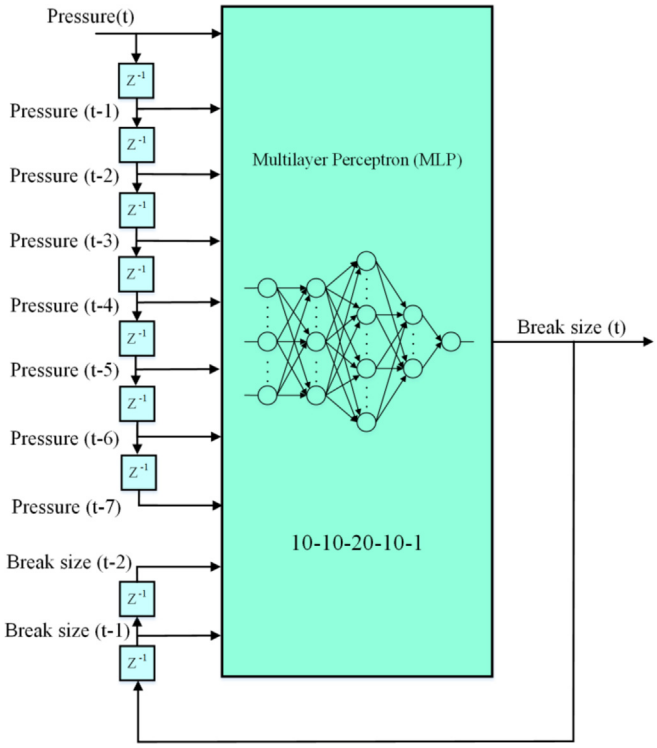

Fig. 9. Detailed structure of the developed NARX neural network for break size estimation.

training transients. The investigation results indicate that 8 s is the optimum training duration of transient condition to estimate the break sizes using time-dependent depressurization patterns (first 10 s of LOCA scenarios in the developed database is related to steady-state condition).

Based on the result of the parametric studies, a NARX neural network with five layers is developed for break size estimation in Bushehr NPP. Input layer consists of eight pressure nodes, two feedbacks from the output layer, and a bias (−1). First node in the input layer receives instantaneous pressure signal from the RPV and next seven nodes receive this pressure signal at previous time steps. Also, the feedbacks from the output layer feed the estimated

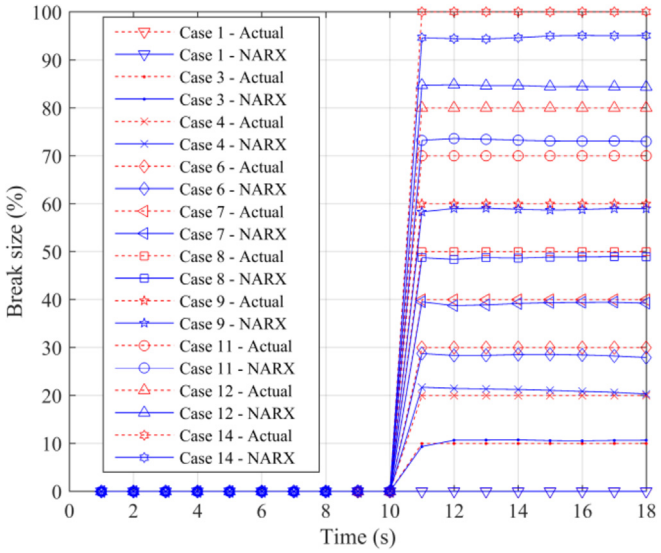

Fig. 10. Estimated and actual break sizes for the training data sets.

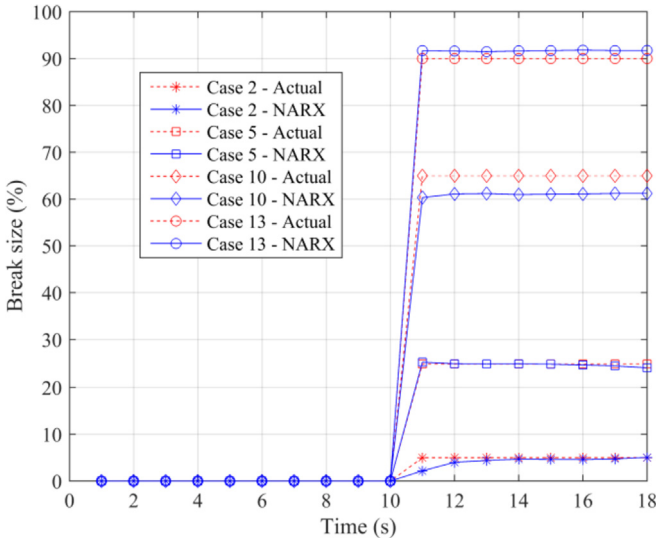

Fig. 11. Estimated and actual break sizes for the validation and testing data sets.

Table 1
Estimated break sizes and relative errors.

Case No.	Data type	Actual break size (%)	Estimated break size (%)	Error[a] (%)	Relative error[b] (%)
1	Training	0	0.02	0.02	–
2	Testing	5	4.30	0.70	14.00
3	Training	10	10.49	0.49	4.90
4	Training	20	21.10	1.10	5.50
5	Validation	25	24.89	0.11	0.44
6	Training	30	28.41	1.59	5.30
7	Training	40	39.25	0.75	1.88
8	Training	50	48.79	1.21	2.42
9	Training	60	58.84	1.16	1.93
10	Validation	65	61.03	3.97	6.11
11	Training	70	73.24	3.24	4.63
12	Training	80	84.58	4.58	5.73
13	Testing	90	91.68	1.68	1.87
14	Training	100	94.81	5.19	5.19
Average error or relative error of all cases		–	–	1.84	4.61

[a] Error is calculated by |(estimated value)-(actual value)|.
[b] Relative error is calculated by |((estimated value)-(actual value))/(actual value)|×100.

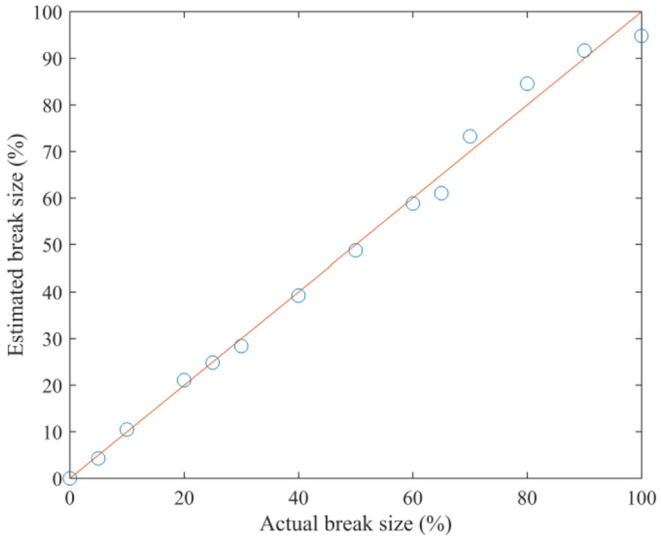

Fig. 12. Actual and average estimated break sizes for the all cases of the database.

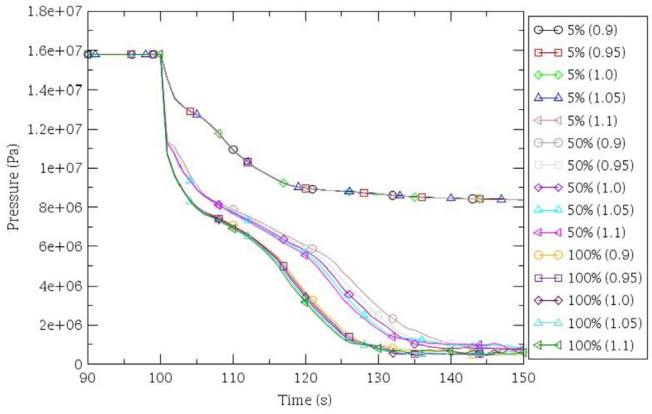

Fig. 13. Time trend of RPV pressure for cases with 5%, 50%, and 100% break areas and different discharge coefficients.

break size into the input layer with delay. Hidden layers have 10-20-10 structure, and output layer has a single neuron which represents the estimated break size. Detailed structure of the developed NARX neural network is presented in Fig. 9.

5. Results and discussion

A standard EBP algorithm with batch learning mode is used to minimize error function of NARX neural network, composed of neurons with sigmoidal activation functions. Training process stops when the NARX neural network has the minimum estimation error for validation data sets, to eliminate over-fitting problem. In Fig. 10, real-time estimated break sizes by NARX neural network for the training data sets are illustrated. Also, estimated break sizes for the testing and validation data sets, which are not used in the training process of NARX neural network, are presented in Fig. 11. The results indicate that NARX neural network is able to estimate the size of LOCAs from the beginning of the transient, even for untrained scenarios. For quantitative comparison of the actual and estimated break sizes, average of estimated break sizes for a transient is defined as follows:

$$D_{average} = \frac{1}{T}\sum_{t=1}^{T} d(t) \tag{9}$$

In Table 1, average value of the estimated break sizes, errors, and relative errors are presented for all cases. Because of rapid and large depressurization in case of large breaks, smaller breaks have smaller errors. The results of NARX neural network for estimation of the untrained cases are in good agreement with the actual break sizes. NARX neural network is able to accurately find a general solution for break size estimation problem in real-time, using a limited number of training cases. Average of estimated break sizes versus their actual values are illustrated in Fig. 12 for all cases.

For evaluation of the sensitivity of NARX estimations to uncertainties in break discharge coefficient of Henry-Fauske critical flow model, same break areas with default discharge coefficient (1.0) are modeled by RELAP5 code with four different discharge coefficients (0.9, 0.95, 1.05, and 1.1). Time-dependent pressure signal is calculated for all break sizes with different discharge

Table 2
Estimated break sizes and relative errors for different discharge coefficients.

Case No.	Actual break size (%)	Discharge coefficients											
		0.9			0.95			1.05			1.1		
		Estimated break size (%)	Error[a] (%)	Relative error[b] (%)	Estimated break size (%)	Error[a] (%)	Relative error[b] (%)	Estimated break size (%)	Error[a] (%)	Relative error[b] (%)	Estimated break size (%)	Error[a] (%)	Relative error[b] (%)
1	0	0.02	0.02	–	0.02	0.02	–	0.02	0.02	–	0.02	0.02	–
2	5	3.63	1.37	27.40	4.12	0.88	17.60	4.37	0.63	12.60	4.42	0.58	11.60
3	10	10.17	0.17	1.70	10.38	0.38	3.76	10.68	0.68	6.81	10.75	0.75	7.46
4	20	20.97	0.97	4.87	21.08	1.08	5.39	21.21	1.21	6.06	21.22	1.22	6.08
5	25	24.59	0.41	1.65	24.53	0.47	1.87	24.91	0.09	0.38	24.99	0.01	0.04
6	30	28.25	1.75	5.84	28.32	1.68	5.59	28.49	1.51	5.03	28.49	1.51	5.03
7	40	38.29	1.71	4.27	39.04	0.96	2.41	39.95	0.05	0.13	40.28	0.28	0.70
8	50	46.37	3.63	7.27	47.92	2.08	4.16	49.99	0.01	0.01	50.00	0.00	0.01
9	60	52.58	7.42	12.37	55.40	4.60	7.66	63.25	3.25	5.41	67.33	7.33	12.21
10	65	56.68	8.32	12.80	61.28	3.72	5.72	71.01	6.01	9.24	77.99	12.99	19.98
11	70	65.28	4.72	6.75	69.76	0.24	0.34	86.83	16.83	24.04	91.82	21.82	31.17
12	80	74.38	5.62	7.03	82.82	2.82	3.53	89.65	9.65	12.06	94.91	14.91	18.64
13	90	82.44	7.56	8.40	89.93	0.07	0.08	95.74	5.74	6.37	99.40	9.40	10.45
14	100	91.73	8.27	8.27	93.16	6.84	6.84	105.59	5.59	5.59	113.54	13.54	13.54
Average error of all cases		–	3.71	8.36	–	1.85	5.00	–	3.66	7.21	–	6.02	10.53

[a] Error is calculated by |(estimated value)-(actual value)|.
[b] Relative error is calculated by |((estimated value)-(actual value))/(actual value)|×100.

coefficients, and it is illustrated for cases with 5%, 50%, and 100% break areas in Fig. 13. Based on the studies on duration of training transients, first 8 s of 56 transients (14 scenarios with 4 different break discharge coefficients) are selected, and the pressure signals are used as inputs of the developed NARX neural network. The results in Table 2 show that, error and relative error are increased by increasing deviations from default break discharge coefficient (1.0) of the training cases in Table 1. This sensitivity study highlights the importance of uncertainties in the developed databases by TH modeling. To the authors' knowledge, no study is performed to determine uncertainty of the predicted pressure in LOCAs or uncertainty of the break size estimation methods. However, uncertainty of predicted peak clad temperature (PCT) in LOCAs are extensively analyzed in the literature [23–26]. Therefore, a complete uncertainty study, including identification and ranking of important variables, is necessary to determine the effect of different TH variables on pressure variation in LOCAs, and consequently on estimated break sizes by NARX neural network.

6. Conclusion

This study deals with feasibility of implementation of NARX neural networks for break size estimation of LOCAs in NPPs. Previous studies used static approaches, e.g. feed-forward neural networks, which employ time-integrated value of TH parameters and rely on independent firing algorithms such as reactor scram signal. NARX neural network is able to directly deal with the time-dependent signals for dynamic estimation of break sizes in real-time.

In this study, NARX neural network, trained by EBP algorithm, is employed to estimate break sizes of LOCAs in Bushehr NPP. The database used for training and testing process of NARX neural network is developed using simulation of Bushehr NPP by RELAP5 code. The results show that NARX neural network is able to accurately find a general solution for break size estimation problem using a limited number of training cases.

The developed NARX neural network will be implemented in break size estimation module of the Tracker in the AMST designed for Bushehr NPP to assist operators in planning appropriate accident management countermeasures during LOCAs. Break size estimation is necessary for timely planning operator actions to recover core heat removal by adequate water injection to replace leak flow rate. In future studies, the break sizes which are estimated by NARX neural network together with location of the breaks which will be categorized by fuzzy classifiers, are used for precise determination of the initiating event by Tracker of the AMST. Then, Predictor of the AMST will predict progress path of the accident using TH modeling by MELCOR code. Finally, Decision-support of the AMST will provide available operator actions in different time windows based on TH predictions.

References

[1] M. Marseguerra, E. Zio, Identification of a line break by a neural network methodology, Ann. Nucl. Energy 21 (1994) 249–258, 1994/04/01.
[2] P. Baraldi, F. Di Maio, M. Rigamonti, E. Zio, R. Seraoui, Clustering for unsupervised fault diagnosis in nuclear turbine shut-down transients, Mech. Syst. Signal Process. 58–59 (2015) 160–178, 2015/06/01/.
[3] Z.-Q. Wang, C.-H. Hu, X.-S. Si, E. Zio, Remaining useful life prediction of degrading systems subjected to imperfect maintenance: application to draught fans, Mech. Syst. Signal Process. 100 (2018) 802–813, 2018/02/01/.
[4] T.V. Santosh, A. Srivastava, V.V.S. Sanyasi Rao, A.K. Ghosh, H.S. Kushwaha, Diagnostic system for identification of accident scenarios in nuclear power plants using artificial neural networks, Reliab. Eng. Syst. Saf. 94 (2009) 759–762, 3//.
[5] S.J. Lee, P.H. Seong, Computational Intelligence in Nuclear Applications: lessons Learned and Recent DevelopmentsA dynamic neural network based accident diagnosis advisory system for nuclear power plants, Prog. Nucl. Energy 46 (2005) 268–281, 2005/01/01.
[6] D.Y. Kim, K.H. Yoo, J.H. Kim, M.G. Na, S. Hur, C.H. Kim, Prediction of leak flow rate using fuzzy neural networks in severe post-LOCA circumstances, IEEE Trans. Nucl. Sci. 61 (2014) 3644–3652.
[7] S.H. Park, J.H. Kim, K.H. Yoo, M.G. Na, Smart sensing of the RPV water level in NPP severe accidents using a GMDH algorithm, IEEE Trans. Nucl. Sci. 61 (2014) 931–938.
[8] M. Saghafi, M.B. Ghofrani, Accident management support tools in nuclear power plants: a post-Fukushima review, Prog. Nucl. Energy 92 (2016) 1–14, 9//.
[9] EPRI, Severe Accident Management Guidance Technical Basis Report, Volumes 2: The Physics of Accident Progression, Palo Alto, CA, 2012.
[10] M.G. Na, S.H. Shin, D.W. Jung, S.P. Kim, J.H. Jeong, B.C. Lee, Estimation of break location and size for loss of coolant accidents using neural networks, Nucl. Eng. Des. 232 (2004) 289–300, 8//.
[11] K. Mo, S.J. Lee, P.H. Seong, A dynamic neural network aggregation model for transient diagnosis in nuclear power plants, Prog. Nucl. Energy 49 (2007) 262–272, 4//.
[12] M.G. Na, W.S. Park, D.H. Lim, Detection and diagnostics of loss of coolant accidents using support vector machines, IEEE Trans. Nucl. Sci. 55 (2008) 628–636.
[13] S.H. Lee, Y.G. No, M.G. Na, K.I. Ahn, S.Y. Park, Diagnostics of loss of coolant accidents using SVC and GMDH models, IEEE Trans. Nucl. Sci. 58 (2011) 267–276.
[14] D. Roverso, Plant diagnostics by transient classification: the aladdin approach, Int. J. Intell. Syst. 17 (2002) 767–790.
[15] M. Saghafi, M. Ghofrani, Introduction of a research project on development of accident management support tool for BNPP (WWER-1000) based on the lessons learned from Fukushima accident, in: Presented at the International Experts Meeting on Strengthening Research and Development Effectiveness in the Light of the Accident at the Fukushima Daiichi Nuclear Power Plant Vienna, Austria, 2015.
[16] M. Saghafi, M.B. Ghofrani, F. D'Auria, Development and qualification of a thermal-hydraulic nodalization for modeling station blackout accident in PSB-VVER test facility, Nucl. Eng. Des. 303 (2016) 109–121, 7//.
[17] M. Saghafi, M.B. Ghofrani, F. D'Auria, Application of FFTBM with signal mirroring to improve accuracy assessment of MELCOR code, Nucl. Eng. Des. 308 (2016) 238–251, 2016/11/01/.
[18] M. Saghafi, F. Yousefpour, K. Karimi, S.M. Hoseyni, Determination of PAR configuration for PWR containment design: a hydrogen mitigation strategy, Int. J. Hydrogen Energy 42 (2017) 7104–7119, 2017/03/09/.
[19] L. Tsungnan, B.G. Horne, C.L. Giles, S.Y. Kung, What to remember: how memory order affects the performance of NARX neural networks, in: Neural Networks Proceedings, 1998. IEEE World Congress on Computational Intelligence. The 1998 IEEE International Joint Conference on vol. 2, 1998, pp. 1051–1056.
[20] L. Tsungnan, B.G. Horne, P. Tino, C.L. Giles, Learning long-term dependencies in NARX recurrent neural networks, IEEE Trans. Neural Network. 7 (1996) 1329–1338.
[21] M. Boroushaki, M.B. Ghofrani, C. Lucas, Identification of a nuclear reactor core (VVER) using recurrent neural networks, Ann. Nucl. Energy 29 (2002) 1225–1240, 7//.
[22] A. Petruzzi, M. Cherubini, F. D'Auria, Thirty years' experience in RELAP5 applications at GRNSPG & NINE, Nucl. Technol. 193 (2016) 47–87.
[23] T. Takeda, ROSA/LSTF test and RELAP5 code analyses on PWR 1% vessel upper head small-break LOCA with accident management measure based on core exit temperature, Nucl. Eng. Technol. 50 (8) (2018) 1412–1420, 2018/08/10/.
[24] T. Takeda, I. Ohtsu, Uncertainty analysis of ROSA/LSTF test by RELAP5 code and PKL counterpart test concerning PWR hot leg break LOCAs, Nuclear Engineering and Technology 50 (2018) 829–841, 2018/08/01/.
[25] J.M. Izquierdo, J. Hortal, M. Sanchez Perea, E. Meléndez, C. Queral, J. Rivas-Lewicky, Current status and applications of integrated safety assessment and simulation code system for ISA, Nuclear Engineering and Technology 49 (2017) 295–305, 2017/03/01/.
[26] S.W. Lee, B.D. Chung, Y.-S. Bang, S.W. Bae, Analysis of uncertainty quantification method by comparing Monte-Carlo method and Wilks' formula, Nuclear Engineering and Technology 46 (2014) 481–488, 2014/08/01/.